A HIGH RESOLUTION ATLAS OF THE GALACTIC PLANE AT 12 μm AND 25 μm

STEPHAN D. PRICE
Geophysics Directorate, Phillips Laboratory

ROSE M. KORTE, REBECCA S. SAMPLE, AND JOHN P. KENNEALY
Mission Research Corporation

ROBERT A. GONSALVES
Electro-Optics Center, Tufts University

ABSTRACT High resolution images of the 12 μm and 25 μm IRAS survey data from each HCON crossing the Galactic Plane are being created for those regions that the original IRAS processing labeled as confused. This encompasses the area within 100° longitude of the Galactic Center and within 3° to 10° of the Plane. The procedures used to create the images preserve the spatial resolution inherent in the IRAS instrument. The images are separated into diffuse and point source components and candidate sources are extracted from the point source image after non-linear spatial sharpening. Fluxes are estimated by convolving the candidate sources with the point response function and cross-correlating with the original point source image. A source is considered real if it is seen on at least two HCONs with a rather generous flux match but a stringent position criterion. A number of fields spanning a range of source densities from low to high have been examined. Initial analysis indicates that the imaging and extraction works quite well up to a source density of about 100 sources per square degree or down to roughly 0.8 Janskys.

INTRODUCTION

The present effort to improve the resolution of the IRAS data products arises from an interest in using such observations to study the structure of the Galaxy. Chester (1986) has shown that at a 12 μm limiting sensitivity of 0.4 Jy, IRAS could detect the moderately bright infrared beacons at least to the Galactic Center. However, previous studies of the properties of the inner Galaxy using the IRAS data (e.g., the shape of the bulge and distribution of AGB stars by Habing et al. (1985) and Habing (1986) and the warping of the Plane derived by Djorgovsky and Sosin (1989)) have discarded the IRAS Point Source Catalog (PSC) (Version 2 1988) data along the Galactic Plane as unreliable due to confusion, precisely in the region most sensitive to the distribution parameters sought. Weinberg (1992a, 1992b) argued that a color-selected sample of objects could be chosen from the PSC which were both bright enough that the PSC completely

S. Terebey and J. Mazzarella (eds.), *Science with High-Spatial Resolution Far Infrared Data*, 45–54, 1994, Jet Propulsion Laboratory, Pasadena, CA.

sampled them and of sufficiently uniform luminosity to trace the mass distribution. From this sample, Weinberg concluded that (1992a) the inner Galaxy was barred rather than having a 4 Kpc ring and (1992b) there was no evidence for a mid-infrared Galactic Bulge. Canterna et al. (private communication), on the other hand, found several different populations of objects in the direction of $l = 30°$ based upon color and apparent scale height and concluded that major constituents of the inner Galaxy were inadequately sampled due to confusion.

We have processed the IRAS survey data to obtain 12 μm and 25 μm images along the Galactic Plane which preserve the inherent spatial resolution of the IRAS instrument. Sources are extracted from each HCON image based on a signal-to-noise criterion. The source lists from the three HCONs are matched with a rather loose flux criterion and a more stringent position criterion. Based on the dLogN/dLog S vs Log S plots, the current processing seems to work well up to source densities of about 100 per square degree. This is some two to four times higher than the practical limit to the PSC. For two moderate density fields, one in the Plane at $l, b \sim (35°, -0.4°)$, the other at the edge of the Galactic Bulge $(l, b \sim 335.4°, 2.4°)$ the "completeness" of the source counts were extended from 2.5 Jy in the PSC to 0.6-0.8 Jy. While the flux agreement between the PSC and the current processing is, in general, quite good, some notable exceptions exist where we have resolved sources that the PSC processing has combined into a single object.

PROCESSING

Initially, our intent was to super-resolve the IRAS survey data on the Galactic Plane with the Filtered Entropy Restoration described by Kennealy et al. (1987), Korte et al. (1989) and Gonsalves et al. (1990). Since this approach uses Fourier transform multiplications for the filtering required by the restoration, it is much faster than the equivalent matrix multiplications used by IPAC's YORIC or Gull and Skilling's MEMSYS. The Filtered Entropy Restoration produces comparable resolution and intensity distributions as the more complex algorithms and is computationally much faster, an important factor given the volume of data to be processed. However, in order for the Fourier Transform based procedure to work at best fidelity, the IRAS "footprint" data has to be projected onto a rectilinear grid with a routine that "whitens" the image resulting in an isoplanatic response function.

Since the primary objective of this effort is to enumerate and quantify the discrete sources down to relatively low signal-to-noise in the high density regions along the Galactic Plane, we subsequently decided it best to extract sources at the regridded stage and use the multiple images from the different HCONs to improve reliability of the flux estimates and confidence in the derived source lists. Sources are extracted from each of the three HCON grids and a two-out-of- three confirmation is used. In contrast, all the data have to be used together to fully realize the resolution enhancement of the maximum entropy procedure. Furthermore, the additional sources we expect to detect are at a signal-to-noise of five to 15 and the resolution of maximum entropy enhancement is known to vary as an inverse function of signal-to-noise (Narayan and Nityananda, 1986).

IMAGE GENERATION

IPAC has provided us with IRAS survey footprint data covering the Galactic Plane in roughly 6° × 6° fields. Each plate of these regions is divided into four overlapping quadrants covering 3.5° × 3.5°. Scan data in these fields are sorted by scan angle and SOP into three groups. Scans with nearly the same scan angle and SOPs closely spaced in time form a group which usually, but not always, corresponds to an HCON. Noise is estimated for each detector by high-pass filtering the data, then iteratively adjusting the rms value by rejecting deviations greater than 2.8σ. The high-pass filter is a Wiener filter which extracts the high-frequency noise component from the data stream of each detector scan. The resulting noise compares favorably with that determined with other methods such as the zero sum filter described in the *IRAS Explanatory Supplement* (1988).

The data from each detector scan are separated into a low frequency or background component and a point or small extended source component. The in-scan background is estimated by a lower bound numerical fitting procedure using a ten sample support. Thus, variations with coherency spanning a width of three detectors or greater than 2′ are included in the background file; more rapid variations are put into a high frequency file. Residual striping is estimated by comparing the in-scan averages in the background file with the cross scan profiles. These baselines are removed. Since a lower bound is used (a few negative points are allowed) the result is biased for the noisy channels; the high frequency values are slightly too large and the background is somewhat too low. The bias adjustment in the background image compensates for the bias in this file.

A background and a source image is created for each quadrant by interpolating the data to an 876 × 876 point grid of 14.4 arc-second pixels. At each grid point, i_m, the brightness, f_g, is calculated by a minimum mean square error interpolation of the nearest twelve data values, d_k, from the irregularly spaced scans. The weights used in the interpolation are such that the resulting image is "whitened" to a uniform model isoplanatic response function, h_m . The model response is an average of the response functions of the largest detectors in the array, made even and symmetric by reflecting the leading response about the median peak to eliminate the tails, then averaging the result of folding the mean response function about the in-scan and cross-scan axes centered on the function. The end product is symmetric about any line drawn through the center of the function. The calculation of the interpolation weights requires the solution of a twelfth-order matrix equation involving the statistical averages of $d_k d_j$ and $d_k i_m$. In essence each scan is convolved with the transpose of the applicable point source response function centered on the cross-scan offset of the grid point in question. The detector response functions, h_d, are those of Moshir (private communication) which are described in the *Explanatory Supplement to the IRAS Faint Source Survey* (Moshir et al. 1992). Weights are assigned to the result proportional to the inverse of the noise of the detector that generated the data point. This 3 × 4 matrix is multiplied by the inverse matrix of the detector response centered on a data point and the transpose centered on the grid point (both suitably weighted by the noise) convolved with a model response.

Mathematically:

$$f_g = (h_d h_d^t + \mathrm{NSR})^{-1} h_m h_d^t F_d,$$

where NSR is a local noise-to-signal ratio and F_d is the vector of twelve data values. There is a slight amount of smoothing to the extent that h_m is slightly larger than h_d for some of the detectors.

The background and source images are added to produce the total image for the quadrant field. A noise grid is also generated based on the weighted averages of the noises multiplied by the whitening matrix.

SOURCE EXTRACTION

An iterative mean square error (mse) gradient image enhancement routine with a positivity constraint is used to sharpen or increase the resolution of the source image. If the stellar fluxes of amplitude a_i are distributed with a position variable x_i such that

$$s(x) = \sum a_i \delta(x - x_i)$$

which is related to the observed source map by

$$d(x) = s(x) * p(x) + n(x)$$

then the sharpening algorithm is

$$\begin{aligned}
s_n &= n^{th} \text{ estimate of } s(x) \\
&= s_{n-1} + \alpha g(x) > 0 \\
\alpha &= \text{step size} = \frac{\int v(x) e(x) dx}{\int v^2(x) dx} \\
v(x) &= g(x) * p(x) \\
g(x) &= \text{mse gradient} = -2\, e(x) * p(x) \\
e(x) &= \text{error} = d(x) - s_{n-1}(x) * p(x)
\end{aligned}$$

Potential sources are at the positions of the peaks of positive excursions from the local background in the sharpened source image. The source lists are subsequently thresholded to be greater than a local signal-to-noise ratio of 4.5. The SNR value was empirically chosen based on eliminating spurious sources in several fields of moderately high source density.

Fluxes are estimated by cross-correlating the positions of the extracted source convolved with the model response function and the match-filtered source image.

$$\begin{aligned}
z(x) &= \text{match-filtered source image} = d(x) * p(x) \\
d(x) &\approx s(x) * p(x) \quad \text{(plus noise)} \\
z(x) &\approx s(x) * p(x) * p(-x) = s(x) * r(x)
\end{aligned}$$

where $r(x)$ is the autocorrelation function of $p(x)$. Since

$$s(x) = \sum a_i \delta(x - x_i),$$
$$z(x) \approx \sum a_i r(x - x_i),$$

which is the flux-weighted sum of the autocorrelation functions centered on the positions of the extracted sources. We evaluate $z(x)$ at the locations, x_k, and solve

$$z(x_k) = \sum a_i r(x_k - x_i) \text{ for the } a_i\text{'s.} \quad (1)$$

In crowded regions, the flux errors for overlapping sources couple with the position errors. We combine these errors by calculating a multiple-parameter Cramer-Rao bound using the Fisher information matrix. The errors are bounded in that they can be no smaller than the Cramer-Rao bound. The local signal-to-noise is increased by the ratio of the square root of the maximum in the autocorrelated response function to the peak input value. In the present case, the gain is about 6.7 for well-isolated sources. Part of this gain comes from smoothing the source image with a matched filter. The rest arises from the fact that the autocorrelation function used in the parameter estimation spans three to four samples of in-scan data from four to five detectors in an HCON. The autocorrelation is a weighted co-addition of these data points which, if the noise is uncorrelated, will improve the signal-to-noise. The "noise" due to confusion decreases this gain by an inverse function of the area common to overlapping sources.

A flux criterion and the distance between candidate sources were used in matching sources from different HCONs. The position uncertainties are well represented by Gaussian distributions; the procedures used to image sharpen the uncertainty distribution from the convolution of a Gaussian with a unit response (CGU) described in the *IRAS Explanatory Supplement* (1988) and by Fowler and Rolfe (1982). A source was included in the Galactic Plane catalog if a position match was found for at least two of the three HCONs and the flux measured on HCON1 was within a factor of two of that from HCON2; no flux criterion was used for matches with HCON3 sources. The output from the matches are positions, fluxes, the errors in these quantities, the SNR, and correlation coefficients derived from the match. The 12 μm and 25 μm lists are band-merged using a position criterion similar to that for the HCON matching. The individual HCON lists are examined for possible matches in the missing color if no band merge has occurred. If such a match is found, it is included in the final source list and appropriately annotated.

RELIABILITY AND COMPLETENESS

It is difficult to estimate the reliability and completeness of the sources detected by these procedures, as comparisons with internal and external source lists are limited. The source selection criteria on flux and number of times observed are certainly less restrictive than those used to create the PSC. On the other hand,

the position matching is significantly tighter in the cross-scan direction. At the moment, our best estimates are inferential and qualitative. The reliability and completeness should be acceptably high because:

- for 24 $3.5° \times 3.5°$ fields we detect >95% of the PSC FQAL=3 sources, and more than half these fields have >98% association rate in the high density regions. There are no significant differences between our positions and those from the PSC. The linear regression between our fluxes and those from the PSC have a slope of 1 and an intercept of 0 within the respective errors. The standard deviation in the fit tends to be higher than the 5% calibration accuracy given in the Explanatory Supplement. This is traced to a broadening of the distribution at the fainter end of the regression and a few outliers where we resolve what the PSC classifies as a single source.
- the log N vs log S plots to fainter levels are consistent with the brighter counts from the PSC. The slopes of the log N vs log S plots are steeper, with physically more plausible values than that derived from the PSC alone. A typical set of flux vs density diagrams is shown in Figure 1. Figure 1a is the result derived from the PSC, while Figure 1b is that from the present study's Galactic Plane Catalog (GPC) for the same field.
- the differential flux vs density plots turn over sharply below the estimated completeness level, as seen below in Figure 2. A cursory examination of a few fields indicates that the source lists may be reliable and complete up to a source density of about 100 objects per square degree or down to a flux of about 0.8-1.0 Jy at 12 μm and 0.6-0.8 Jy at 25 μm. A noise-dominated distribution increases the slope as observed for the low density region shown in Figure 3. Scans from two of the HCONs for this field are, unfortunately, nearly parallel and phased such that the noisy detectors overlap, producing an overabundance of coincidences on noise peaks.

There are several analyses by which we hope to quantify reliability and completeness. The University of Wyoming is using MEMSYS-5 to super-resolve a number of IRAS AO's near the Galactic Plane. We will compare the survey results with this data set, which is independent both in acquisition and the method of restoration. We will use the mini-survey to compare the results of a two-out-of-three criterion with that derived from a larger number of images. We will randomize the positions of two of the HCONs for several fields to estimate the number of coincidental agreements.

RESULTS

For the 24 fields surveyed, the effort described in this paper produces from two to four times as many sources as in the PSC. If the qualitative arguments regarding completeness and reliability are valid, then we have indeed achieved our objective of improving the source counts along the Galactic Plane. Log_{10} (F_{12} /F_{25}) plots for an area in the Galactic Plane at $l \sim 35°$ and at the edge of the bulge ($l \sim -4.6°$, $l \sim 2.3°$) show a distribution sharply peaked near a value

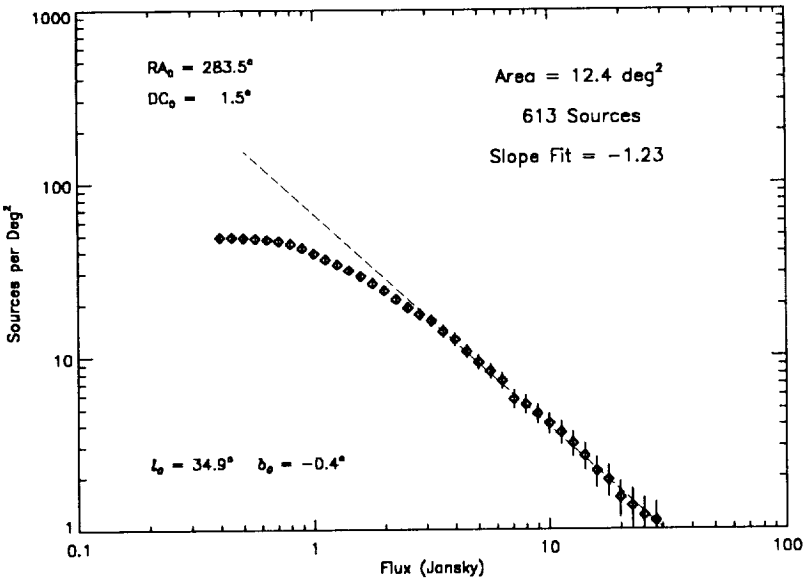

Figure 1a. Distribution of PSC Sources

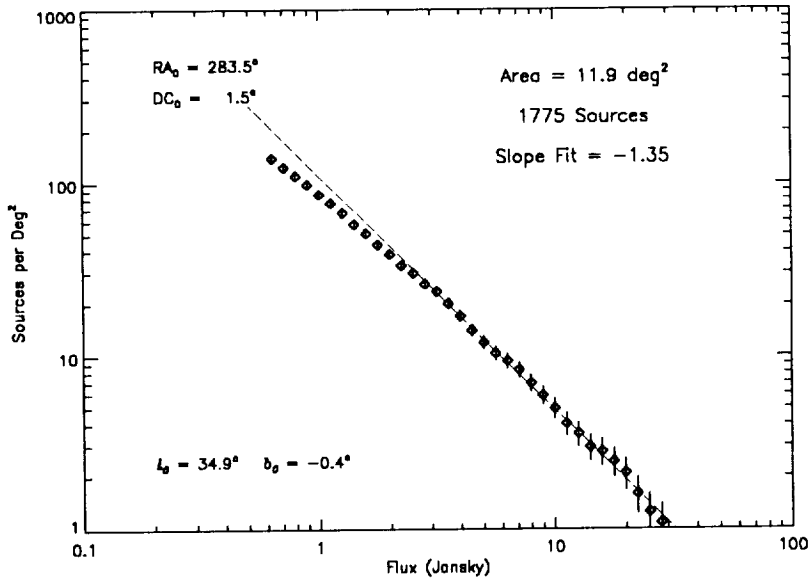

Figure 1b. Distribution of GPC Sources

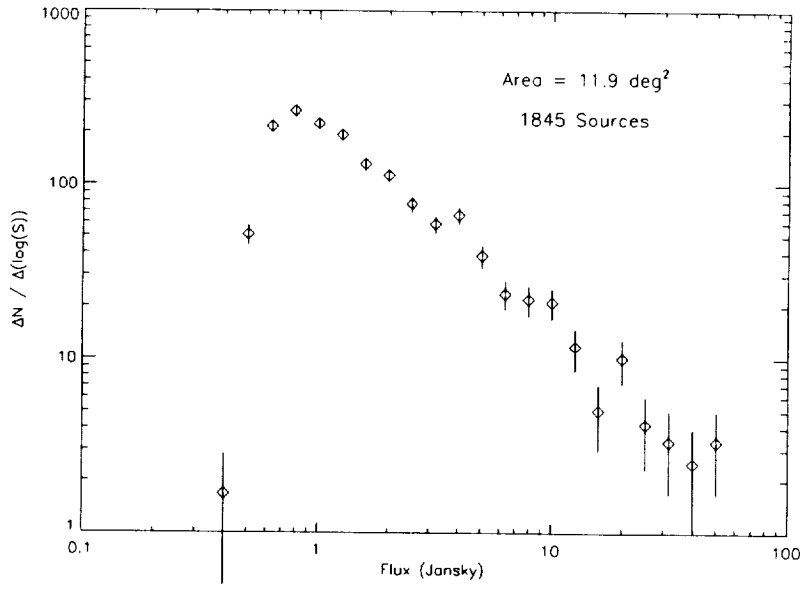

Figure 2a. Differential Band 1 (12μm) Distribution

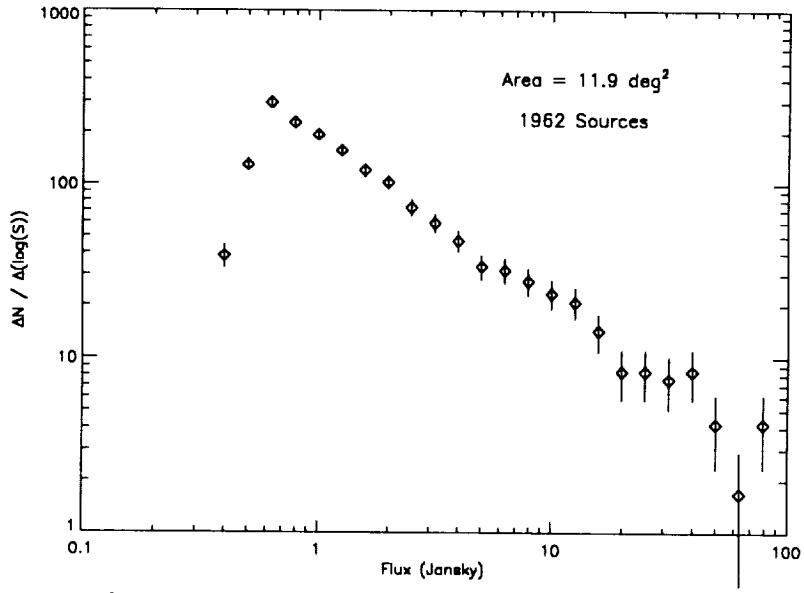

Figure 2b. Differential Band 2 (25μm) Distribution

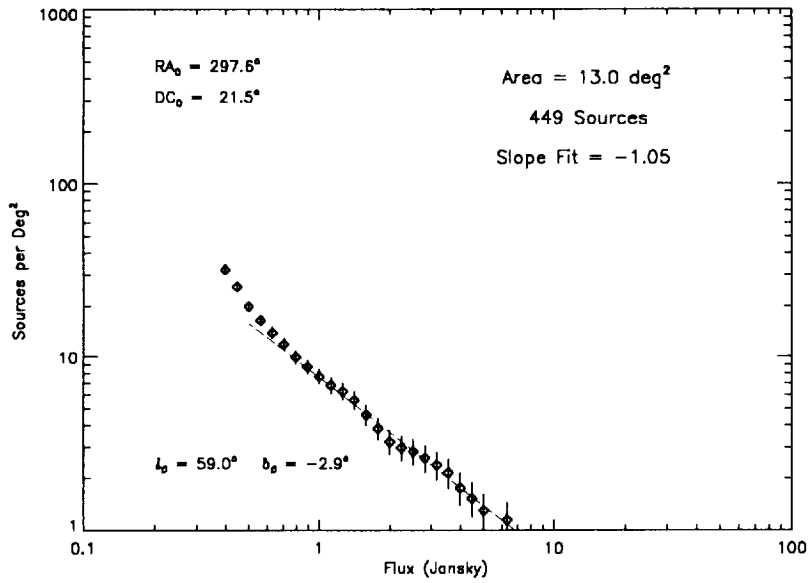

Figure 3. Low-density Band 1 data

of 0. This is similar to what Weinberg (1992b) found for the variable AGB stars he used as structure tracers. Unfortunately, this value for the peak is almost forced by the fact that most of the stars in a given field will have fluxes near the cutoff and the sensitivities at 12 μm and 25 μm are nearly the same.

REFERENCES

Chester, T.J. 1986, in *Light on Dark Matter*, ed. F.P. Israel, Dordrecht: Reidel, 3

Djorgovski, S., and Sosin, C. 1989, *ApJ*, **341**, L13

Fowler, J.W., and Rolfe, E.G. 1982, *Journal of Astronautical Sci.*, **Vol. XXX, No. 4**, pp. 385-402

Gonsalves, R.A., Kennealy, J.P., Korte, R.M., and Price, S.D. 1990, in *Maximum Entropy and Bayesian Methods*, ed. P.F Fougere, Kluweter Academic Press (Neth), 369

Habing, H.J. 1986, in *Light on Dark Matter*, ed. F.P. Israel, Dordrecht: Reidel, 329

Habing, H.J., Olnon, F.M., Chester, T. Gillett, F.C., Rowan-Robinson, M., and Neugebauer, G. 1985, *A&A*, **152**, L1

IRAS Catalogs and Atlases: Explanatory Supplement. 1988, ed. C.A. Beichman, G. Neugebauer, H.J. Habing, P.E. Clegg, and T.J. Chester (Washington, DC: GOP)

Kennealy, J.P., Korte, R.M., Gonsalves, R.M., Lyons, T.D., Price, S.D., LeVan, P.D., and Aumann, H.H. 1987, in it Advances in Image Processing, Proc. SPIE, **804**, 16

Korte, R.M., Kennealy, J.P., Gonsalves, R.A., and Wong, C. 1989, "Analysis of IR Celestial Survey Experiments, AF Geophysics Lab. Technical Report, *GL-TR-89-0265*

Moshir, M., et al. 1989, *Explanatory Supplement to the IRAS Faint Source Survey* (Pasadena: JPL)

Narayan, R., and Nityananda, R. 1986, *ARA&A*, **24** , 127

Weinberg, M. 1992a, *ApJ*, **384** , 81

Weinberg, M. 1992b, *ApJ*, **392**, L67